majority of the existing studies were limited to normal-strength materials and concentric loading. Thus, further studies are required on the effect of high-strength materials and eccentric loading.

2. TIME-DEPENDENT NUMERICAL ANALYSIS

To investigate the long-term effect on the structural behavior of composite columns, time-dependent numerical analysis was performed using the age-adjusted effective modulus method (Bazant 1972) and relaxation solution procedure (Bresler and Selna 1964; Gilbert 1988; Bradford and Gilbert 1990; Adrian and Triantafillou 1992; and Morino et al. 1996). To predict the creep coefficient $\phi_{cr}(t)$ and shrinkage strain $\varepsilon_{sh}(t)$ of concrete, the modified ACI 209R-92 model (ACI 1997; and Huo et al. 2001) was used [Eq. (1)]. In the modified model, the characteristics of high-strength concrete were taken into account: higher development of creep and shrinkage at early ages; and lower values of ultimate creep and shrinkage.

$$\phi_{cr}(t) = \frac{(t-t_0)^{0.6}}{K_{cr} + (t-t_0)^{0.6}} \phi_{cru} \left(\gamma_{cr,t0} \cdot \gamma_{cr,RH} \cdot \gamma_{cr,vs} \cdot \gamma_{cr,s} \cdot \gamma_{cr,\psi} \cdot \gamma_{cr,\alpha} \cdot \gamma_{cr,fc} \right) \quad (1a)$$

$$\varepsilon_{sh}(t) = \frac{(t-t_c)}{K_{sh} + (t-t_c)} \varepsilon_{shu} \left(\gamma_{sh,tc} \cdot \gamma_{sh,RH} \cdot \gamma_{sh,vs} \cdot \gamma_{sh,s} \cdot \gamma_{sh,\psi} \cdot \gamma_{sh,c} \cdot \gamma_{sh,\alpha} \cdot \gamma_{sh,fc} \right) \quad (1b)$$

where t = time, t_0 = loading age, and t_c = initial moist curing duration. ϕ_{cru} = ultimate creep coefficient, and ε_{shu} = ultimate shrinkage strain. $\gamma_{cr,t0}$, $\gamma_{cr,RH}$, $\gamma_{cr,vs}$, $\gamma_{cr,s}$, $\gamma_{cr,\psi}$, $\gamma_{cr,\alpha}$, $\gamma_{cr,fc}$ = creep correction factors for loading age (t_0), ambient relative humidity (RH), volume-to-surface ratio (v/s), slump (s), fine aggregate ratio (ψ), air content (α), and concrete strength (= 1.18 – 0.0065f_c'), respectively. $\gamma_{sh,tc}$, $\gamma_{sh,RH}$, $\gamma_{sh,vs}$, $\gamma_{sh,s}$, $\gamma_{sh,\psi}$, $\gamma_{sh,c}$, $\gamma_{sh,\alpha}$, $\gamma_{sh,fc}$ = shrinkage correction factors for initial moist curing duration (t_c), ambient relative humidity, volume-to-surface ratio, slump, fine aggregate ratio, cement content (c), air content, and concrete strength (= 1.20 – 0.0073f_c'), respectively. K_{cr}, K_{sh} = adjustment factors for early-age creep (= 12 – 0.0725f_c') and shrinkage (= 45 – 0.3626f_c').

For the numerical analysis, a fiber model method was used considering the strain-compatibility and the confinement effect of the steel section and transverse bars (Kim et al. 2012 and 2014). The full analysis procedure consisted of three steps: 1) long-term loading on the composite column; 2) analysis of the long-term response; and 3) analysis of the ultimate load capacity after long-term loading.

For verification, the results of the time-dependent numerical analysis were compared with those of a previous experimental study. In the previous experimental study, ultimate load tests were performed after long-term load tests for three concrete-encased steel (CES) columns (C1, C2, and C3) and a concrete-filled steel tube (CFT) column (C4). Table 1 summarizes the properties of the test specimens. By using the measured values of ϕ_{cru} = 1.44, ε_{shu} = 553, and ε_{asu} = 161 (ultimate autogenous shrinkage strain) from the long-term load tests, the time-dependent numerical analysis

was performed. Figs. 1 and 2 show the comparisons of the numerical analysis results with the long-term load test results and ultimate load test results. As shown in the figures, although there was some discrepancy in the long-term behavior, the numerical analysis results (thin lines) generally agreed with the test results (thick solid lines). At t = 147 days, the mean value and standard deviation of the ratios of the numerical analysis result to the test result were 92% and 0.113 for long-term strains, 96% and 0.038 for internal forces, or 107% and 0.037 for peak loads, respectively.

Table 1 Properties of Test Specimens

Specimens		CES			CFT
		C1	C2	C3	C4
Section	Dimensions, $B \times D$ (mm)	180×180	180×180	180×180	180×180
	Gross Area, $A_g = BD$ (mm^2)	32400	32400	32400	32400
Concrete	$f'_{c,28}$ (MPa)	104	104	104	104
Steel	f_{ys} (f_{us}, MPa)	812 (868)	812 (868)	812 (868)	812 (868)
	Steel Shape (b_s/t_s)	H-80×80×15×15 (2.17)	H-80×80×15×15 (2.17)	H-80×80×15×15 (2.17)	□-80×80×15 (10)
	Steel Ratio, $\rho_s = A_s/A_g$ (%)	9.7	9.7	9.7	30.6
Longitudinal Bars	No. and Dia. (f_{yl}, MPa)	4-D10 (474)	4-D10 (474)	4-D10 (474)	-
	Rebar Ratio, $\rho_{sl} = A_l/A_g$ (%)	0.9	0.9	0.9	-
Overall Compressive Strength	Composite Section, P_0 (kN)*	5243.7	5243.7	5243.7	10020.2
	Steel Contribution, P_s/P_0	0.49	0.49	0.49	0.80
Net Column Length, L (mm) (Total Specimen Length, L_k)		980 (980)	980 (2140)	980 (2880)	980 (2880)
Slenderness Ratio, $\lambda = KL_k/r$**		26.1	58.1	76.7	43.7
Transverse Bars	Arrangement (f_{yt}, MPa)	D6@90mm (348)	D6@90mm (348)	D6@90mm (348)	-
	Vol. Ratio, ρ_t	0.98	0.98	0.98	-
Eccentricity of Axial Load, e_0 (mm) (Eccentricity, e_0/D)		0 (0)	0 (0)	30 (0.167)	30 (0.167)
Long-term Load, P_{LT}***		-	$0.4P_u$	$0.4P_u$	$0.4P_u$

* $P_0 = 0.85f'_cA_c + f_{ys}A_s + f_{yl}A_l$

** Effective length factor K = 1, Radius of gyration $r = \sqrt{(0.2E_cI_c + E_sI_s)/(0.2E_cA_c + E_sA_s)}$ (mm, ACI 318-14), $E_c = 3320\sqrt{f'_c} + 6900$ (MPa, ACI 363R), and E_s = 205 GPa.

*** P_u = Short-term ultimate strength predicted by numerical analysis

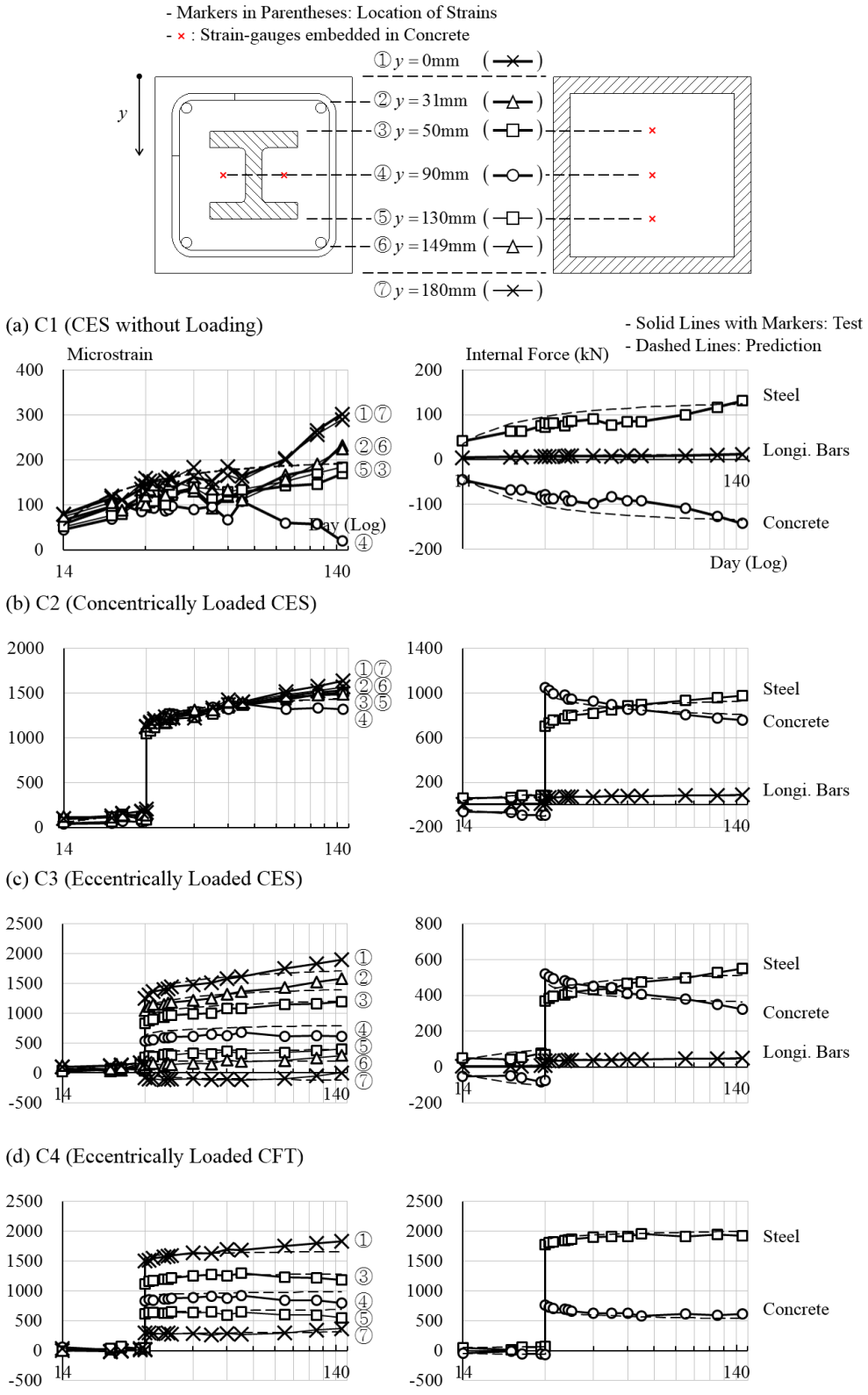

Fig. 1 Strains and Internal Forces of Composite Columns